

6-5-1998

$b \rightarrow S\gamma$ Constraints on the Minimal Supergravity Model with Large $\tan\beta$

Howard Baer
Florida State University

Michal Brhlik
University of Michigan-Ann Arbor

Diego Castano
St. Leo College, castanod@nova.edu

Xerxes Tata
University of Hawaii

Follow this and additional works at: https://nsuworks.nova.edu/cnso_chemphys_facarticles

 Part of the [Physics Commons](#)

NSUWorks Citation

Baer, H., Brhlik, M., Castano, D., & Tata, X. (1998). $b \rightarrow S\gamma$ Constraints on the Minimal Supergravity Model with Large $\tan\beta$. *Physical Review D*, 58, (1), 1 - 20. <https://doi.org/10.1103/PhysRevD.58.015007>. Retrieved from https://nsuworks.nova.edu/cnso_chemphys_facarticles/125

This Article is brought to you for free and open access by the Department of Chemistry and Physics at NSUWorks. It has been accepted for inclusion in Chemistry and Physics Faculty Articles by an authorized administrator of NSUWorks. For more information, please contact nsuworks@nova.edu.

$b \rightarrow s\gamma$ CONSTRAINTS ON THE MINIMAL SUPERGRAVITY MODEL WITH LARGE $\tan\beta$

Howard Baer¹, Michal Brhlik², Diego Castaño³ and Xerxes Tata⁴

¹*Department of Physics, Florida State University, Tallahassee, FL 32306 USA*

²*Randall Laboratory of Physics, University of Michigan, Ann Arbor, MI 48109 USA*

³*Saint Leo College, St. Leo, FL 33574 USA*

⁴*Department of Physics and Astronomy, University of Hawaii, Honolulu, HI 96822, USA*

(February 1, 2008)

Abstract

In the minimal supergravity model (mSUGRA), as the parameter $\tan\beta$ increases, the charged Higgs boson and light bottom squark masses decrease, which can potentially increase contributions from tH^\pm , $\tilde{g}\tilde{b}_j$ and $\tilde{Z}_i\tilde{b}_j$ loops in the decay $b \rightarrow s\gamma$. We update a previous QCD improved $b \rightarrow s\gamma$ decay calculation to include in addition the effects of gluino and neutralino loops. We find that in the mSUGRA model, loops involving charginos also increase, and dominate over tW , tH^\pm , $\tilde{g}\tilde{q}$ and $\tilde{Z}_i\tilde{q}$ contributions for $\tan\beta \gtrsim 5 - 10$. We find for large values of $\tan\beta \sim 35$ that most of the parameter space of the mSUGRA model for $\mu < 0$ is ruled out due to too large a value of branching ratio $B(b \rightarrow s\gamma)$. For $\mu > 0$ and large $\tan\beta$, most of parameter space is allowed, although the regions with the least fine-tuning (low m_0 and $m_{1/2}$) are ruled out due to too low a value of $B(b \rightarrow s\gamma)$. We compare the constraints from $b \rightarrow s\gamma$ to constraints from the neutralino relic density, and to expectations for sparticle discovery at LEP2 and the Fermilab Tevatron $p\bar{p}$ colliders. Finally, we show that non-universal GUT scale soft breaking squark mass terms can enhance gluino loop contributions to $b \rightarrow s\gamma$ decay rate even if these are diagonal.

I. INTRODUCTION

Models of particle physics including weak scale supersymmetry (SUSY) are amongst the most promising candidates [1] for new physics at the TeV scale. Of this class of models, the minimal supergravity (mSUGRA) model stands out as providing one of the most economic explanations for the diversity of soft supersymmetry breaking terms in the SUSY Lagrangian [2]. In this model [3], supersymmetry is communicated from a hidden sector (whose dynamics leads to the breaking of supersymmetry) to the observable sector (consisting of the fields of the Minimal Supersymmetric Standard Model or MSSM) via gravitational interactions. With the assumption of canonical kinetic terms for scalars in the Lagrangian, this leads to a universal mass m_0 for all scalar particles at some high scale Q , usually taken to be M_{GUT} . At M_{GUT} , gaugino masses and trilinear terms are assumed to unify at $m_{1/2}$ and A_0 , respectively. These parameters, along with the bilinear soft term B , provide boundary conditions for the renormalization group evolution of the various soft terms from M_{GUT} to M_{weak} . Requiring in addition radiative electroweak symmetry breaking leaves a rather small parameter set

$$m_0, m_{1/2}, A_0, \tan\beta \text{ and } sign(\mu), \quad (1.1)$$

from which the entire SUSY particle mass spectrum and mixing parameters may be derived.

The flavor changing neutral current decay of the bottom quark $b \rightarrow s\gamma$ is well known to be particularly sensitive to new physics effects. New weak scale particles (*e.g.*, a chargino \widetilde{W}_i and top squark \widetilde{t}_j) could give loop contributions which would be comparable to the Standard Model (SM) tW^- loop amplitude. Measurements from the CLEO experiment [4] restrict the inclusive $B \rightarrow X_s\gamma$ branching ratio to be $B(B \rightarrow X_s\gamma) = (2.32 \pm 0.57 \pm 0.35) \times 10^{-4}$, where $1 \times 10^{-4} < B(B \rightarrow X_s\gamma) < 4.2 \times 10^{-4}$ at 95% CL. Many analyses have been performed [5–7] which compare theoretical predictions of SUSY models to experimental results.

In a previous report [7], predictions of the $b \rightarrow s\gamma$ decay rate were made as functions of the mSUGRA model parameter space. In this study, a number of QCD improvements were incorporated into the calculation which reduced the inherent uncertainty of the $b \rightarrow s\gamma$ decay rate predictions due to the QCD scale choice from $\sim 25\%$ down to $\sim 9\%$. SUSY contributions to the $b \rightarrow s\gamma$ decay amplitude included tW , tH^+ and $\widetilde{W}_i\widetilde{q}_j$ loops. Results were presented for $\tan\beta = 2$ and 10, and for both signs of μ . For $\mu < 0$, large regions of parameter space were excluded, especially for $\tan\beta = 10$. For $\mu > 0$, all the parameter space scanned was allowed by CLEO data: in fact, for some ranges of parameters, the model predicts values of $B(b \rightarrow s\gamma)$ close to the central value measured by the CLEO Collaboration.

Recently, sparticle mass spectra and sparticle decay branching ratios in the mSUGRA model have been reanalysed for large values of the parameter $\tan\beta$ [8]. In the mSUGRA model, the range of $\tan\beta$ is typically $1.6 \lesssim \tan\beta \lesssim 45 - 50$, where the lower limit depends somewhat on the precise value of m_t . For $\tan\beta \gtrsim 5 - 10$, b and τ Yukawa couplings become non-negligible and can affect the sparticle mass spectrum and decay branching fractions. The upper and lower limits on $\tan\beta$ are set by a combination of requiring a valid solution to radiative electroweak symmetry breaking, and requiring perturbativity of third generation Yukawa couplings between the scales M_{weak} and M_{GUT} . Some optimization of scale choice at which the one-loop effective potential is minimized was found to be needed in Ref. [8] in order to gain stable sparticle and Higgs boson mass contributions. This scale optimization

effectively includes some portion of two-loop corrections to the effective potential [9]. It was shown that the mass of the pseudoscalar Higgs boson A^0 , and the related masses of H^0 and H^+ , suffer a sharp decrease as $\tan\beta$ increases. In addition, the masses of the lighter tau slepton $\tilde{\tau}_1$ and bottom squark \tilde{b}_1 also decrease, although less radically. Naively, one might expect corresponding increases in the loop contributions to $b \rightarrow s\gamma$ decay involving \tilde{b}_1 and H^+ .

Indeed, Borzumati has shown in Ref. [10] that as m_{H^+} decreases, the charged Higgs contribution to $b \rightarrow s\gamma$ decay does increase. However, for large values of $\tan\beta$, the chargino loop contributions increase even more dramatically, and dominate the decay amplitude. She further notes that at intermediate to large $\tan\beta$ values, there is a non-negligible contribution from $\tilde{g}\tilde{q}$ loops.

In this paper, we re-examine constraints on the mSUGRA model from $b \rightarrow s\gamma$ decay at large $\tan\beta$. In doing so, we incorporate several improvements over previous analyses.

- We present our analysis using updated mSUGRA mass predictions for large $\tan\beta$, using a renormalization group improved one-loop effective potential with optimized scale choice $Q = \sqrt{\overline{m_{\tilde{t}_L}} \overline{m_{\tilde{t}_R}}}$. We use an updated value of top mass $m_t = 175$ GeV.
- We include in this analysis contributions from $\tilde{g}\tilde{q}_j$ and $\tilde{Z}_i\tilde{q}_j$ loops. These contributions require knowledge of the full squark mixing matrices, and hence an improved calculation of renormalization group evolution of soft SUSY breaking parameters.
- As in Ref. [7], we include the dominant next-to-leading order (NLO) virtual and bremsstrahlung corrections to the operators mediating $b \rightarrow s\gamma$ decay at scale $Q \sim m_b$. In addition, we include NLO RG evolution of Wilson coefficients between scales M_W and m_b . We also include appropriate renormalization group evolution of Wilson coefficients at high scales $Q > M_W$ for tW , tH^+ and $\tilde{W}_i\tilde{q}_j$ loops following the procedure of Anlauf [11]. The corresponding RG evolution of Wilson coefficients for $\tilde{g}\tilde{q}_j$ and $\tilde{Z}_i\tilde{q}_j$ loops is not yet available.
- We compare our results to recent calculations at large $\tan\beta$ of the neutralino relic density and direct dark matter detection rates for the mSUGRA model.

In Sec. II of this paper, we present some details of our calculations, especially those regarding the inclusion of $\tilde{g}\tilde{q}_j$ and $\tilde{Z}_i\tilde{q}_j$ loops. In Sec. III, we present QCD improved results for the $b \rightarrow s\gamma$ branching fraction in mSUGRA parameter space for large $\tan\beta$. In this section, we also make comparisons with cosmological and collider search expectations. In Sec. IV, we relax some of the assumptions of the mSUGRA framework to see whether $\tilde{g}\tilde{q}_j$ loops can become large or even dominant. This question is important when considering the model dependence of our results.

II. CALCULATIONAL DETAILS

The calculation of the width for $b \rightarrow s\gamma$ decay proceeds by calculating the loop interaction for $b \rightarrow s\gamma$ within a given model framework, *e.g.*, mSUGRA, at some high mass scale $Q \sim M_W$, and then matching to an effective theory Hamiltonian given by

$$H_{eff} = -\frac{4G_F}{\sqrt{2}}V_{tb}V_{ts}^* \sum_{i=1}^8 C_i(Q)O_i(Q), \quad (2.1)$$

where the $C_i(Q)$ are Wilson coefficients evaluated at scale Q , and the O_i are a complete set of operators relevant for the process $b \rightarrow s\gamma$, given, for example, in Ref. [12]. All orders approximate QCD corrections are included via renormalization group resummation of leading logs (LL) which arise due to a disparity between the scale at which new physics enters the $b \rightarrow s\gamma$ loop corrections (usually taken to be $Q \sim M_W$), and the scale at which the $b \rightarrow s\gamma$ decay rate is evaluated ($Q \sim m_b$). Resummation then occurs when we solve the renormalization group equations (RGE's) for the Wilson coefficients

$$Q \frac{d}{dQ} C_i(Q) = \gamma_{ji} C_j(Q), \quad (2.2)$$

where γ is the 8×8 anomalous dimension matrix (ADM), and

$$\gamma = \frac{\alpha_s}{4\pi} \gamma^{(0)} + \left(\frac{\alpha_s}{4\pi}\right)^2 \gamma^{(1)} + \dots \quad (2.3)$$

The matrix elements of the operators O_i are finally calculated at a scale $Q \sim m_b$ and multiplied by the appropriately evolved Wilson coefficients to gain the final decay amplitude. The dominant uncertainty in this leading-log theoretical calculation arises from an uncertainty in the scale choice Q at which effective theory decay matrix elements are evaluated. Varying Q between $\frac{m_b}{2}$ to $2m_b$ leads to a theoretical uncertainty of $\sim 25\%$.

Recently, next-to-leading order QCD corrections have been completed for $b \rightarrow s\gamma$ decay. These include *i*) complete virtual corrections [13] to the relevant operators O_2 , O_7 and O_8 which, when combined with bremsstrahlung corrections [14,13] results in cancellation of associated soft and collinear singularities; *ii*) calculation of $\mathcal{O}(\alpha_s^2)$ contributions to the ADM elements $\gamma_{ij}^{(1)}$ for $i, j = 1 - 6$ (by Ciuchini *et al.* [15]), for $i, j = 7, 8$ by Misiak and Münz [16], and for $\gamma_{27}^{(1)}$ by Chetyrkin, Misiak and Münz [17]. In addition, if two significantly different masses contribute to the loop amplitude, then there can already exist significant corrections to the Wilson coefficients at scale M_W . In this case, the procedure is to create a tower of effective theories with which to correctly implement the RG running between the multiple scales involved in the problem. The relevant operator bases, Wilson coefficients and RGE's are given by Cho and Grinstein [18] for the SM and by Anlauf [11] for the MSSM. The latter analysis includes contributions from just the tW , tH^- and $\tilde{t}_i \tilde{W}_j$ loops (which are the most important ones). We include the above set of QCD improvements (with the exception of $\gamma_{27}^{(1)}$, which has been shown to be small [17]) into our calculations of the $b \rightarrow s\gamma$ decay rate for the mSUGRA model.

The contributions to $C_7(M_W)$ and $C_8(M_W)$ from $\tilde{g}\tilde{q}$ and $\tilde{Z}_i\tilde{q}$ loops (SUSY contributions to $C_2(M_W)$ are suppressed by additional factors of g_s^2) have been presented in Ref. [5], although some defining conventions must be matched between Ref. [5] and Ref. [11] and Ref. [13]. The only complication is that the squark mixing matrix Γ which enters the couplings must be derived. To accomplish this, we incorporate the following procedure into our program for renormalization group running.

- We first calculate the values of all running fermion masses in the SM at the mass scale M_Z . From these, we derive the corresponding Yukawa couplings h_u , h_d and h_e for

each generation, and construct the corresponding Yukawa matrices $(h_u)_{ij}$, $(h_d)_{ij}$ and $(h_e)_{ij}$, where $i, j = 1, 2, 3$ runs over the 3 generations. We choose a basis that yields flavor diagonal matrices for $(h_d)_{ij}$ and $(h_e)_{ij}$, whereas the CKM mixing matrix creates a non-diagonal matrix $(h_u)_{ij}$ [19].

- The three Yukawa matrices are evolved within the MSSM from $Q = M_Z$ up to $Q = M_{GUT}$ and the values are stored. We use 1-loop RGEs except for the evolution of gauge couplings.
- At $Q = M_{GUT}$, the matrices $(Ah_u)_{ij}$, $(Ah_d)_{ij}$ and $(Ah_e)_{ij}$ are constructed (assuming $A(M_{GUT}) = A_0 \times \mathbf{1}$). The squark and slepton mass squared matrices $(M_k^2)_{ij}$ are also constructed, where $k = \tilde{Q}, \tilde{u}, \tilde{d}, \tilde{L}$ and \tilde{e} . These matrices are assumed diagonal at $Q = M_{GUT}$ with entries $m_0^2 \delta_{ij}$.
- The $(Ah)_{ij}$ and $(M_k^2)_{ij}$ matrices are evolved along with the rest of the gauge/Yukawa couplings and soft SUSY breaking terms between M_Z and M_{GUT} iteratively via Runge-Kutta method until a stable solution is found. The entire solution requires the simultaneous solution of 134 coupled RGE's (with some slight redundancy). We use 1-loop RGEs except for the evolution of gauge couplings.
- At $Q = M_Z$, the 6×6 d -squark mass squared matrix is constructed. Numerical diagonalization of this matrix yields the squark mass mixing matrix Γ which is needed for computation of the $\tilde{g}\tilde{q}$ and $\tilde{Z}_i\tilde{q}$ loop contributions.

At this point, the Wilson coefficients $C_7(M_W)$ and $C_8(M_W)$ can be calculated and evolved to $Q \sim m_b$ as described above, so that the $b \rightarrow s\gamma$ decay rate can be calculated [7].

As an example, we show in Fig. 1 the calculated contributions to the Wilson coefficient $C_7(M_W)$ versus $\tan\beta$ for the mSUGRA point $m_0, m_{1/2} = 100, 200$ GeV, $A_0 = 0$ and $\mu > 0$. In frame *a*), we show contributions from $\tilde{W}_i\tilde{q}$ loops, as well as from tW and tH^- . The tW contribution is of course constant, while the tH^- contribution is of the same sign, and increasing slightly in magnitude. The various contributions from chargino loops increase roughly linearly with $\tan\beta$ at a much faster rate, and thus form the dominant components of the $b \rightarrow s\gamma$ decay amplitude. In the case shown, there are several large negative as well as positive contributions, so that significant cancellations take place. The sum of all chargino loop contributions is shown by the dotted curve. In frame *b*) we show the contributions to $C_7(M_W)$ from different $\tilde{g}\tilde{q}$ loops. These contributions vary with $\tan\beta$ as well and are comparable to corresponding contributions from chargino loops. The sum of all gluino loop contributions is shown by the dotted curve; in this case, however, the cancellation amongst the various loop contributions is nearly complete.

In frame *c*), we show the individual and summed contributions from $\tilde{Z}_i\tilde{q}$ loops. These also increase with $\tan\beta$ but, as expected, are tiny compared to the $\tilde{W}_i\tilde{q}$ and $\tilde{g}\tilde{q}$ loop contributions. The sum is again shown by the dotted curve. Here, the cancellations are not as complete as in the gluino loop case due to the Higgsino interactions of the neutralinos which increase with $\tan\beta$.

III. NUMERICAL RESULTS AND IMPLICATIONS

A. Constraints from $b \rightarrow s\gamma$ decay

Our first numerical results for $B(b \rightarrow s\gamma)$ decay are shown in Fig. 2, where we plot the branching fraction versus $\tan\beta$ for the mSUGRA point $m_0, m_{1/2} = 100, 200$ GeV, $A_0 = 0$ and for a) $\mu < 0$ and b) $\mu > 0$. The SM value, after QCD corrections, is $B(b \rightarrow s\gamma) = 3.2 \pm 0.3 \times 10^{-4}$, where the error comes from varying the scale choice $\frac{m_b}{2} < Q < 2m_b$ [7,20]. The SM result is denoted by the dot-dashed line, and of course does not vary with $\tan\beta$. If we include in addition the contribution from the tH^- loop, then we obtain the dotted curves, which always increase the value of $B(b \rightarrow s\gamma)$. For this parameter space point, including the tH^- loop always places the value of $B(b \rightarrow s\gamma)$ above the CLEO 95% CL excluded region of $B(b \rightarrow s\gamma) < 4.2 \times 10^{-4}$.

If we include the full contribution of supersymmetric particles to the computation of $B(b \rightarrow s\gamma)$, then we arrive at the solid curves in Fig. 2. For the $\mu < 0$ case in frame a), the SUSY loops increase the branching fraction, which increases with $\tan\beta$, so that the CLEO restriction on $B(b \rightarrow s\gamma)$ severely constrains the mSUGRA model for large $\tan\beta$. For the frame b) case with $\mu > 0$, the SUSY loop contributions generally act to decrease the branching fraction, so that much of the parameter space is allowed for moderate values of $\tan\beta$. Ultimately, as $\tan\beta$ increases, the decrease in $B(b \rightarrow s\gamma)$ becomes so severe that the mSUGRA model becomes in conflict with the CLEO lower 95% CL bound that $B(b \rightarrow s\gamma) > 1 \times 10^{-4}$, so that for this particular mSUGRA point, all values of $\tan\beta > 21$ are excluded for the particular choice of mSUGRA parameters.

In Figure 3, we show the main result of this paper: the contours of constant $B(b \rightarrow s\gamma)$ in the m_0 vs. $m_{1/2}$ parameter plane for large $\tan\beta = 35$, for $A_0 = 0$ and for a) $\mu < 0$ and b) $\mu > 0$. The contours are evaluated at a renormalization scale choice $Q = m_b$. The region marked by TH is disallowed by theoretical considerations: either electroweak symmetry is not properly broken (the large m_0 , small $m_{1/2}$ region) or the lightest neutralino \tilde{Z}_1 is not the lightest SUSY particle (LSP). For small m_0 , the light tau slepton $\tilde{\tau}_1$ becomes so light that in the TH region, $m_{\tilde{\tau}_1} < m_{\tilde{Z}_1}$. The region denoted by EX is excluded by LEP2 constraints which require that the light chargino mass $m_{\tilde{W}_1} > 80$ GeV.

In frame a), we see the value of $B(b \rightarrow s\gamma)$ is large throughout the entire parameter space plane. The region with small values of m_0 and $m_{1/2}$ which is most favored by fine-tuning considerations [21] is in the most severe violation of the CLEO constraint. The region below the dotted contour is in violation of the CLEO 95% CL bound for *all* choices of renormalization scale $\frac{m_b}{2} < Q < 2m_b$. Thus, SUSY models allowed by CLEO for $\tan\beta = 35$ and $\mu < 0$ would be required to have $m_{\tilde{g}} > 1470$ GeV (at $m_0, m_{1/2} = 1000, 600$ GeV) and $m_{\tilde{q}} > 1600$ GeV (for $m_0, m_{1/2} = 320, 800$ GeV).

In frame b) for $\mu > 0$, we see that the values of $B(b \rightarrow s\gamma)$ are uniformly *below* the SM value, and so usually in better agreement with the CLEO measured value of $B(b \rightarrow s\gamma) = 2.32 \pm 0.67 \times 10^{-4}$ (where errors have been combined in quadrature). In fact, we note that the region with $m_{1/2} \simeq 500$ GeV agrees with the CLEO central value for $B(b \rightarrow s\gamma)$! This region corresponds to parameter space points with $m_{\tilde{g}} \simeq 1200$ GeV, and $m_{\tilde{W}_1} \simeq 400$ GeV. In this frame, the entire plane shown, except the region below the dotted contour, is *allowed* by the CLEO constraint. The region below the dotted contour falls below the CLEO 95% CL value of $B(b \rightarrow s\gamma) > 1 \times 10^{-4}$ for all values of scale choice $\frac{m_b}{2} < Q < 2m_b$. This is again the region most favored by fine-tuning. In this plane, $m_{\tilde{g}} \gtrsim 525$ GeV and $m_{\tilde{q}} \gtrsim 575$ GeV.

Up to this point, we have only shown results for a constant value of $A_0 = 0$. In Figure 4, we show contours of constant $B(b \rightarrow s\gamma)$ in the m_0 vs. A_0 plane for $m_{1/2} = 200$ GeV, for $\tan\beta = 35$ and a) $\mu < 0$ and b) $\mu > 0$. For frame a), we see that the branching fraction can change by typically a factor of 2 over the parameter range shown, with most of the variation occurring for changes in m_0 , instead of with A_0 . The entire plane shown in frame a) is excluded by the CLEO bound. In frame b), for $\mu > 0$, the branching fraction can change by up to a factor of ~ 4 over the plane shown, again with most of the variation coming due to changes in m_0 . In this case, the region to the left of the dotted contour is excluded by the CLEO bound for all choices of renormalization parameter $\frac{m_b}{2} < Q < 2m_b$.

B. Comparison with relic density and direct detection rates for neutralino dark matter

An important constraint on the mSUGRA model comes from implications for the relic density of dark matter in the universe. The idea here is that in the very early universe, the LSP (the lightest neutralino) was a constituent of the matter and radiation assumed to be in thermal equilibrium at some very high temperature. As the universe expanded and cooled, the LSP's could no longer be produced, although they could still annihilate with one another. Upon further expansion, the neutralino flux dropped to such low levels that further annihilations would rarely occur, and a relic abundance of neutralinos was locked in. These relic LSP's could make up the bulk of dark matter in the universe today.

The neutralino relic density is calculable as a function of mSUGRA model parameter space [22]. The relic density is usually parametrized in terms of Ωh^2 , where $\Omega = \rho/\rho_c$, ρ is the relic density, ρ_c is the critical closure density of the universe ($\rho_c = \frac{3H_0^2}{8\pi G_N}$) and $H = 100h$ km/sec/Mpc is the scaled Hubble constant with $0.5 \lesssim h \lesssim 0.8$. A value of $\Omega h^2 > 1$ implies a universe with age less than 10 billion years, in conflict with the ages of the oldest stars. If $\Omega h^2 < 0.025$, then the relic density of neutralinos cannot even account for the dark matter required by galactic rotation curves. Some popular cosmological models that account for the COBE cosmic microwave background measurements as well as structure formation in the universe actually prefer a mixed dark matter (MDM) universe [23], with a matter density ratio of 0.3/0.6/0.1 for a hot dark matter/cold dark matter/baryonic matter mix. In this case, values of $\Omega h^2 \simeq 0.15 - 0.4$ are preferred.

In Fig. 5, we show contours of constant relic density Ωh^2 . The region to the right of the solid $\Omega h^2 = 1$ contour is excluded by the age of the universe constraint, while the region below the dotted contour has $\Omega h^2 < 0.025$. The region between the dashed-dotted contours is favored by a MDM universe. The region excluded by CLEO data is below the solid contour labelled $b \rightarrow s\gamma$. In frame a), we see that combining the two constraints allows only a small patch of allowed parameter space with $m_{1/2} > 700$ GeV and $300 \lesssim m_0 \lesssim 600$ GeV. Over almost all of this region, the relic density $\Omega h^2 > 0.4$. In frame b), the $b \rightarrow s\gamma$ excluded region hardly intersects with the MDM region, so that large regions of parameter space are favorable for cosmology as well as for CLEO constraints!

In Fig. 5 we also plot one contour for expected rates for direct detection of neutralino dark matter via cryogenic dark matter detectors [24]. The calculations have been performed for neutralino scattering from a ^{73}Ge detector. Current experiments are sensitive to detection rates of 1-10 events/day/kg of detector. The goal of such experiments is to achieve

a sensitivity of ~ 0.01 events/kg/day by about the year 2000. Towards this end, we show the 0.01 event/kg/day contour in the m_0 vs. $m_{1/2}$ plane; below the contour the event rates exceed the 0.01/kg/day benchmark. In frame *a*), we see that the region accessible to direct neutralino detection coincides with the region with very large $B(b \rightarrow s\gamma)$ rates well beyond the CLEO 95% CL limit. However, in frame *b*), for $\mu > 0$, there exists a significant region with large direct detection rates, which is allowed by the CLEO constraint, and is also in the favorable cosmological region!

C. Implications for collider experiments

The LEP2 e^+e^- collider is expected to reach a peak CM energy of $\simeq 195$ GeV, which should allow SM Higgs bosons of mass $m_{H_{SM}} \lesssim 95$ GeV to be explored. For the $\tan\beta = 35$ value shown in Fig. 5, the light Higgs scalar $m_h \gtrsim 110$ GeV over the entire m_0 vs. $m_{1/2}$ plane shown. Hence, for these values of $\tan\beta$, we would expect no Higgs signals to be seen at LEP2. The reach of LEP2 via $\tilde{\tau}_1\tilde{\tau}_1$ and $\tilde{W}_1\tilde{W}_1$ searches is shown by the dashed contour just above the region marked EX. This contour is defined by requiring $m_{\tilde{W}_1} = 95$ GeV and $m_{\tilde{\tau}_1} = 85$ GeV. For both cases of $\mu < 0$ and $\mu > 0$ shown in Fig. 5, the LEP2 sparticle reach falls below both the $B(b \rightarrow s\gamma)$ excluded region, and below the $\Omega h^2 = 0.025$ contours. If we accept the mSUGRA model literally, then the prediction is that LEP2 should see no evidence for either a Higgs or SUSY if $\tan\beta \simeq 35$.

The Fermilab Tevatron $p\bar{p}$ collider is expected to operate at $\sqrt{s} = 2$ TeV in Run 2, and to amass ~ 2 fb $^{-1}$ of integrated luminosity by use of the Main Injector (MI). Ultimately, experiments hope to acquire ~ 25 fb $^{-1}$ of integrated luminosity under the TeV33 program. Recently completed calculations of the reach of the Tevatron MI for mSUGRA at large $\tan\beta \simeq 35$ show a maximal reach in $m_{1/2}$ to $\simeq 150$ GeV in the \cancel{E}_T +jets channel [25]. A similar reach has been calculated for TeV33, and finds points with $m_{1/2} \simeq 175$ accessible. Comparing these regions to Fig. 5 shows that, like LEP2, the reach of Tevatron MI and TeV33 are below both the $B(b \rightarrow s\gamma)$ excluded contour and the $\Omega h^2 = 0.025$ contour, making discovery of SUSY particles highly unlikely for mSUGRA if $\tan\beta$ is large. Over much of the parameter space plane in frame *b*) of Fig. 5, however, $m_h \lesssim 120$ GeV, which (optimistically) corresponds to the maximal reach for h at TeV33. Hence, if mSUGRA is correct and $\tan\beta \simeq 35$, then TeV33 experiments may see a hint of the Higgs boson in their data sample. Of course, the entire large $\tan\beta$ parameter space shown should be easily visible in at least the jets+ \cancel{E}_T channel at the CERN LHC, even with modest integrated luminosity.

IV. MODEL DEPENDENCE OF $\tilde{g}\tilde{q}$ LOOP CONTRIBUTIONS

It is well known that within the mSUGRA framework the chargino loop gives the dominant SUSY contribution to the amplitude for the decay $b \rightarrow s\gamma$. This can also be seen from Fig. 1 where we see that while the contributions from the gluino loops are individually comparable (or even larger!) than those from chargino loops, these cancel out almost completely leaving only a small residual contribution. In contrast, while there is indeed considerable cancellation amongst the various chargino contributions, there is nonetheless a sizeable residue that remains. We may understand the large cancellations among the gluino

contributions in analogy with the familiar GIM cancellation in the SM: indeed such a cancellation would be exact if squarks were precisely degenerate (*i.e.*, the squark mass matrix is proportional to the unit matrix) because we can then, by a unitary transformation, align the squark and quark mass matrices, so that the gluino-squark-quark vertex is exactly flavour diagonal. Within the mSUGRA framework with universal soft breaking squark mass matrices at the unification scale, squarks are indeed (approximately) degenerate, and gluino loop contributions to the flavour violating $b \rightarrow s\gamma$ decay are suppressed. The GIM-like cancellation that we have described above does not occur when Yukawa couplings enter the calculation as occurs, for instance, via the higgsino components of chargino and neutralino loops. In this case, as can be seen from Fig. 1, the cancellation is indeed incomplete (particularly for the chargino where the large top quark Yukawa coupling enters).

These considerations lead us to examine whether the breaking of the degeneracy of the soft SUSY-breaking squark masses at the unification scale so strongly upsets the delicate cancellations that it results in large gluino contributions to the amplitude for $b \rightarrow s\gamma$ decay. Of course, by allowing soft-breaking mass squared matrices with arbitrary off-diagonal entries, it should be possible to get very large flavour violating gluino interactions. The issue that we address, however is whether large gluino contributions are possible even if we choose these soft squark matrices to be diagonal at the unification scale. As we will soon see, the physics of this ansatz is basis-dependent.

To parametrize the breaking of the squark degeneracy we begin by noting that we may always choose a quark basis so that *either* the down or the up type Yukawa couplings are diagonal at the weak scale. We will call these the d - and u - cases, respectively. Next, these couplings are evolved to M_{GUT} , where both up and down Yukawa matrices have off-diagonal components. In the d -case, the down type Yukawa matrices get off-diagonal contributions just from the RGE, while the up type Yukawas start off off-diagonal right at the weak scale; in the u -case, the situation is reversed. Up to now, the choice to work in the u or d cases is purely a matter of convention, and indeed in previous sections we have used the d case. This is, however, no longer the case if we further assume that the soft breaking squark mass squared matrix is diagonal (but not a multiple of the identity) at the GUT scale. This is because the transformation that takes us from the d -case to the u -case does not leave the squark mass squared matrix diagonal (except in the case when this matrix is $m_0^2 \times \mathbf{1}$). The u - and d - cases are thus physically distinct.

We have, therefore, studied these two cases separately. To keep things simple, we split only the b -squarks (t_L splits with b_L , of course) keeping the others degenerate at m_0 . The splitting is given by a single parameter

$$x = (m_{\tilde{b}_i}/m_0)^2,$$

where m_b and m_0 are soft squark masses at the GUT scale. Thus $x = 1$ corresponds to the mSUGRA case. We further consider three possibilities where (i) just \tilde{b}_L , (ii) just \tilde{b}_R and (iii) both \tilde{b}_L and \tilde{b}_R masses are split from those of other squarks.

The results of our calculation of the gluino contribution to $C_7(M_W)$ where the squark degeneracy is broken as described above is shown in Fig. 6 for the d -case labelled d -diagonal, and for the u -case, labelled u -diagonal. In each frame, we have three curves labelled L , R and LR for the cases where just left, just right, and both left and right sbottom soft masses are different from m_0 . In our calculation, we have chosen $m_0 = 500$ GeV, $m_{1/2} = 200$ GeV,

$\tan\beta = 35$, $A_0 = 0$ and $\mu > 0$. We choose a large value of m_0 so that the squark masses are not dominated by $m_{\tilde{g}}$ (in which case splitting due to non-universal soft mass term would be unimportant). Also, for the large value of $\tan\beta$ the bottom Yukawa coupling is significant. The following features are worth noting.

- For $x = 1$ the value of $C_7^{gluino}(M_W)$ is the same for the up and down cases for reasons that we have already explained.
- For non-degenerate squarks, gluino loop effects are significantly larger in the u -case. This may be understood if we recall that in the d -case, the mixing of down type Yukawas at M_{GUT} arises *only* due to RGE.
- Non-degeneracy effects when just the right squarks are split show only small variation with the non-degeneracy parameter x because flavour mixing in the right squark sector is suppressed.
- Somewhat surprising is the fact that despite the large degree of non-degeneracy, the gluino contribution to $C_7(M_W)$, which increases by up to an order of magnitude relative to that in the mSUGRA case, never becomes really large. For our choice of parameters, this may be partly due to the fact that gluinos and squarks are significantly heavier than W and t . This is not the complete reason though. In our computation we find that the three main contributions (from the two sbottoms and the \tilde{s}_L) cancel one another leaving a remainder that is typically smaller than 10-15% of the largest contribution. While this cancellation is much less complete than in the mSUGRA case, we are unable to give a simple argument for why such a cancellation occurs.

Finally, we comment on the neutralino contributions for the case of non-degenerate squarks. We have already noted that cancellations among various chargino contributions are incomplete because of the effect of large higgsino couplings to the $t\tilde{t}$ system. For large values of $\tan\beta$, we may expect a similar effect for neutralinos. We may further guess that this effect is largest in the u -case where flavor mixing does not originate solely in the RGE. We have checked that for values of parameters in Fig. 6 above a small value of $x = 0.0625$, the neutralino contribution to $C_7(M_W)$ is indeed enhanced by a factor of 6-7 above its mSUGRA value, and further, that this enhancement is largely due to incompleteness in the cancellation between various contributions. For very large values of x , $C_7(M_W)$ is about 1.5 times its mSUGRA value, but opposite in sign. We thus conclude that while the neutralino contribution is somewhat sensitive to the splitting of squark masses, it never appears to become very dominant.

To summarize the results of this Section, we see that with our assumptions, gluino contributions to the amplitude for the $b \rightarrow s\gamma$ decay never dominate the SUSY contribution. This contribution may nonetheless be non-negligible even if gluinos and squarks are well beyond the reach of the Tevatron (and its proposed upgrades) as seen in Fig. 6. We emphasize though that our conclusion is special to models where all the flavour violation in the gluino-squark-quark vertex at the GUT scale comes from non-diagonal Yukawa interactions. Larger contributions from gluino loops may be possible in other models.

Note added: After completion of this manuscript, a related paper by Blazek and Raby appeared on the topic of $b \rightarrow s\gamma$ constraints on $SO(10)$ SUSY models at large $\tan\beta$ [26].

Since Ref. [26] adopts a particular $SO(10)$ framework and does not include the radiative electroweak symmetry breaking constraint, comparison of results between the two papers is not straightforward. Also, we have not included $\tilde{t}_L - \tilde{c}_L$ mixing included in Ref. [26] in our evaluation of the chargino loop.

ACKNOWLEDGMENTS

We are grateful to M. Drees and T. ter Veldhuis for helpful conversations and comments. We thank the Aspen Center for Physics for hospitality while a portion of this work was completed. This research was supported in part by the U. S. Department of Energy under grant number DE-FG-05-87ER40319.

REFERENCES

- [1] See, *e.g.*, H. Haber in *Woodlands Superworld*, hep-ph/9308209 (1993).
- [2] See *e.g.*, M. Drees and S. Martin in *Electroweak Symmetry Breaking and New Physics at the TeV Scale*, edited by T. Barklow, S. Dawson, H. Haber and J. Seigrist, (World Scientific) 1995; see also J. Amundson *et al.* in *New Directions for High Energy Physics*, edited by D. G. Cassel, L. Trindle Gennari and R. H. Siemann, (Stanford Linear Accelerator Center, 1996), hep-ph/9609374.
- [3] A. Chamseddine, R. Arnowitt and P. Nath, Phys. Rev. Lett. **49**, 970 (1982); R. Barbieri, S. Ferrara and C. Savoy, Phys. Lett. **B119**, 343 (1982); L.J. Hall, J. Lykken and S. Weinberg, Phys. Rev. **D27**, 2359 (1983).
- [4] M. S. Alam *et al.*, (CLEO Collaboration), Phys. Rev. Lett. **74**, 2885 (1995). Note that recently the ALEPH collaboration (at the International Europhysics Conference on High Energy Physics, Jerusalem, Israel, Aug. 19-26, 1997) has made a preliminary announcement of a measurement of $B(B \rightarrow X_s \gamma) = (3.38 \pm 0.74 \pm 0.85) \times 10^{-4}$. We do not include this preliminary result in our analysis, and caution the reader that some of our conclusions may change if the $b \rightarrow s \gamma$ decay rate turns out to be closer to this ALEPH value.
- [5] S. Bertolini, F. Borzumati, A. Masiero and G. Ridolfi, Nucl. Phys. **B353**, 591 (1991).
- [6] R. Barbieri and G. F. Giudice, Phys. Lett. **B309**, 86 (1993); J. Lopez, D. Nanopoulos and G. Park, Phys. Rev. **D48**, 974 (1993); N. Oshimo, Nucl. Phys. **B404**, 20 (1993); R. Garisto and J. Ng, Phys. Lett. **B315**, 372 (1993); M. Diaz, Phys. Lett. **B322**, 207 (1994); Y. Okada, Phys. Lett. **B315**, 119 (1993); F. Borzumati, Zeit. für Physik **C63**, 291 (1994); P. Nath and R. Arnowitt, Phys. Lett. **B336**, 395 (1994); G. Kane, C. Kolda, L. Roszkowski and J. Wells, Phys. Rev. **D49**, 6173 (1994); F. Borzumati, M. Drees and M. Nojiri, Phys. Rev. **D51**, 341 (1995); V. Barger, M. Berger, P. Ohmann and R. Phillips, Phys. Rev. **D51**, 2438 (1995); F. Bertolini and F. Vissani, Zeit. für Physik **C67**, 513 (1995); J. Lopez, D. Nanopoulos, X. Wang and A. Zichichi, Phys. Rev. **D51**, 147 (1995); J. Wu, R. Arnowitt and P. Nath, Phys. Rev. **D51**, 1371 (1995); B. de Carlos and J. A. Casas, Phys. Lett. **B349**, 300 (1995) and ERRATUM-*ibid* **B351**, 604 (1995).
- [7] H. Baer and M. Brhlik, Phys. Rev. **D55**, 3201 (1997).
- [8] H. Baer, C. H. Chen, M. Drees, F. Paige and X. Tata, Phys. Rev. Lett. **79**, 986 (1997).
- [9] M. Carena, J. Espinosa, M. Quiros and C. Wagner, Phys. Lett. **B355**, 209 (1995); M. Carena, M. Quiros, C.E.M. Wagner, Nucl. Phys. **B461**, 407 (1996); H. Haber, R. Hempfling and A. Hoang, Z. Phys. **C75**, 539 (1997).
- [10] See F. Borzumati, Ref. [6].
- [11] H. Anlauf, Nucl. Phys. **B430**, 245 (1994).
- [12] See, *e.g.*, B. Grinstein, M. J. Savage and M. Wise, Nucl. Phys. **B319**, 271 (1989); A. Ali, in *20th International Nathiagali Summer College on Physics and Contemporary Needs*, Bhurban, Pakistan, 1995, hep-ph/9606324.
- [13] C. Greub, T. Hurth and D. Wyler, Phys. Lett. **B380**, 385 (1996) and Phys. Rev. **D54**, 3350 (1996).
- [14] A. Ali and C. Greub, Z. Phys. **C49**, 431 (1991), Phys. Lett. **B259**, 182 (1991), **287**, 191 (1992) and **361**, 146 (1995); Z. Phys. **C60**, 433 (1993); N. Pott, Phys. Rev. **D54**, 938 (1996);
- [15] M. Ciuchini, E. Franco, G. Martinelli and L. Reina, Nucl. Phys. **B415**, 403 (1994).

- [16] M. Misiak and M. Münz, Phys. Lett. **B344**, 308 (1995).
- [17] K. G. Chetyrkin, M. Misiak and M. Münz, Phys. Lett. **B400**, 206 (1997).
- [18] P. Cho and B. Grinstein, Nucl. Phys. **B365**, 279 (1991).
- [19] H. Arason *et al.*, Phys. Rev. **D46**, 3945 (1992).
- [20] Ref. [17], A. Buras, A. Kwiatkowski and N. Pott, hep-ph/9707482 (1997) and C. Grueb and T. Hurth, hep-ph/9708214 (1997) quote a somewhat higher SM value of $B(b \rightarrow s\gamma)$ than is presented here. The above works include a 3% increase due to non-perturbative effects calculated by M. B. Voloshin, Phys. Lett. **B397**, 275 (1997) plus the corrected value of γ_{27} in their calculations, which conspire to increase the SM decay rate by about 10%. These effects would similarly increase our estimate of the SUSY contributions.
- [21] G. Anderson and D. Castaño, Phys. Lett. **B347**, 300 (1995) and Phys. Rev. **D52**, 1693 (1995); see also K. L. Chan, U. Chattopadhyay and P. Nath, hep-ph/9710473 (1997).
- [22] For a recent review, see G. Jungman, M. Kamionkowski and K. Griest, Phys. Rep. **267**, 195 (1996). See also M. Drees and M. Nojiri, Phys. Rev. **D47**, 376 (1993). The result shown here are from H. Baer and M. Brhlik, Phys. Rev. **D53**, 597 (1996). Further references are included in these reports.
- [23] See *e.g.*, J. Primack, astro-ph/9707285 (1997).
- [24] H. Baer and M. Brhlik, Phys. Rev. D, in press, hep-ph/9706509.
- [25] H. Baer, C. H. Chen, M. Drees, F. Paige and X. Tata, manuscript in preparation.
- [26] T. Blazek and S. Raby, hep-ph/9712257 (1997).

FIGURES

FIG. 1. We plot the value of the Wilson coefficient $C_7(M_W)$ versus $\tan\beta$, where $m_0, m_{1/2} = 100, 200$ GeV, $A_0 = 0$ and $\mu > 0$. In *a*), we show the contribution from the tW and tH^\pm loops, as well as contributions from various loops containing charginos. The \tilde{q} contribution includes both \tilde{c}_L and \tilde{u}_L squarks. In *b*), we show the corresponding contributions from loops containing gluinos, and in *c*) we show the contributions from loops including neutralinos.

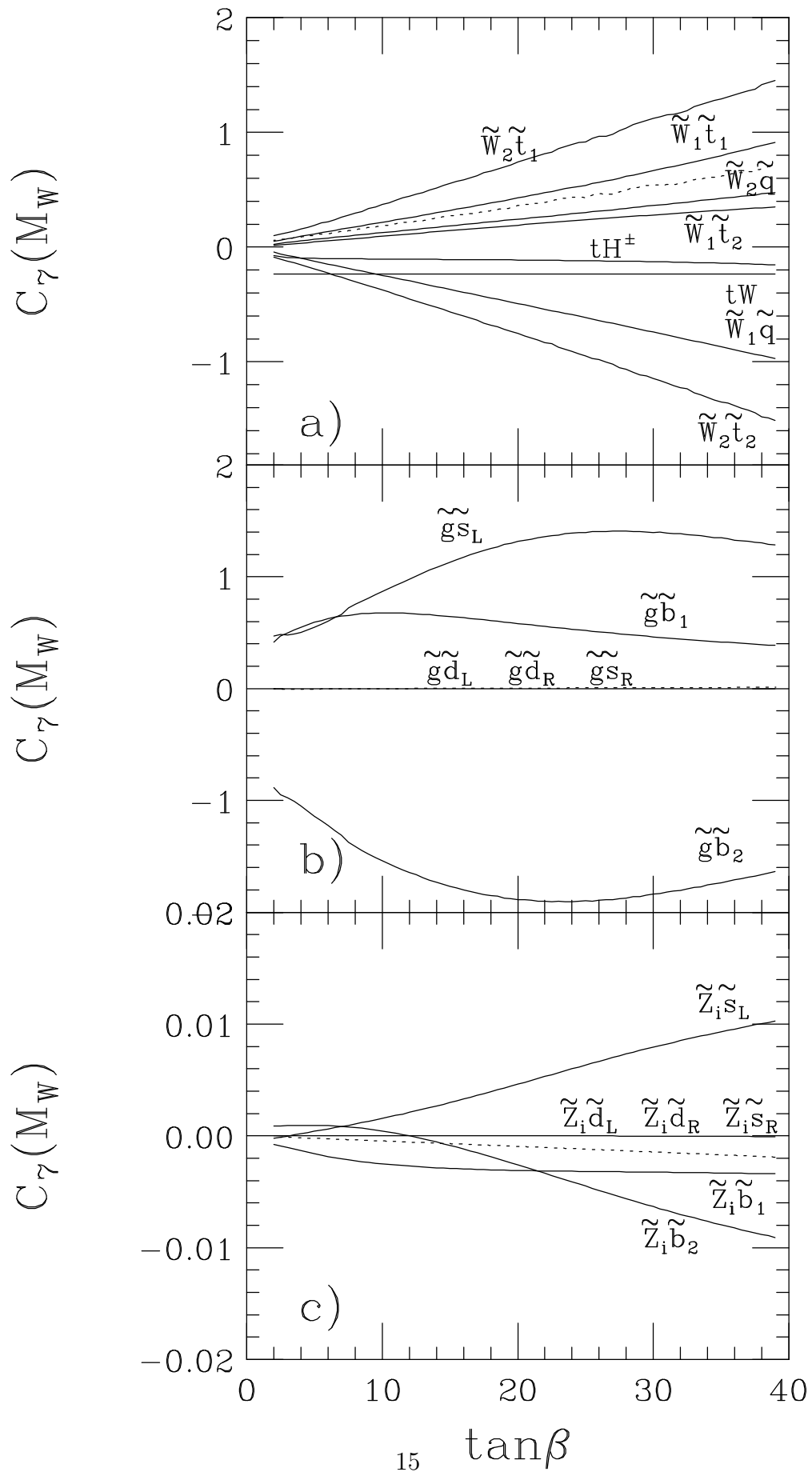
FIG. 2. We show the branching ratio $B(b \rightarrow s\gamma)$ versus $\tan\beta$ for the same parameter space point as in Fig. 1, but with *a*) $\mu < 0$ and *b*) $\mu > 0$. The curves shown are for Standard Model prediction (dot-dashed), SM plus charged Higgs prediction (dots) and the complete SUSY calculation (solid).

FIG. 3. Plot of contours of constant branching ratio $B(b \rightarrow s\gamma)$ in the m_0 vs. $m_{1/2}$ plane, where $\tan\beta = 35$, $A_0 = 0$ and $m_t = 175$ GeV. Each contour should be multiplied by 10^{-4} . Frame *a*) is for $\mu < 0$ and frame *b*) is for $\mu > 0$. The regions labelled by TH (EX) are excluded by theoretical (experimental) considerations. The EX region corresponds to the LEP2 limit of $m_{\tilde{W}_1} > 80$ GeV for a gaugino-like chargino.

FIG. 4. Plot of contours of constant branching ratio $B(b \rightarrow s\gamma)$ in the m_0 vs. A_0 plane, where $\tan\beta = 35$, $m_{1/2} = 200$ GeV and $m_t = 175$ GeV. Each contour should be multiplied by 10^{-4} . Frame *a*) is for $\mu < 0$ and *b*) is for $\mu > 0$.

FIG. 5. Plot of contours of constant neutralino relic density Ωh^2 in the m_0 vs. $m_{1/2}$ plane, where $\tan\beta = 35$, $A_0 = 0$ and $m_t = 175$ GeV. We also show the region excluded by CLEO data on $B(b \rightarrow s\gamma)$ searches (the region below the $b \rightarrow s\gamma$ solid contour). The region accessible to direct neutralino dark matter detectors is below the 10^{-2} contours. The region accessible to LEP2 sparticle searches is below the dashed contour in the lower-left.

FIG. 6. Contributions to $C_7(M_W)$ from the gluino- squark loop for the d -case and u -case discussed in the text as a function of the non-degeneracy parameter $x = \frac{m_{\tilde{b}_i}^2}{m_0^2}$. The curves labelled L , R and LR refer to the cases where just $m_{\tilde{b}_L}$, $m_{\tilde{b}_R}$ and both $m_{\tilde{b}_{L,R}}$ are different from the universal squark mass m_0 at the unification scale. For reference, we remind the reader that $C_7^{SM} = -0.23$



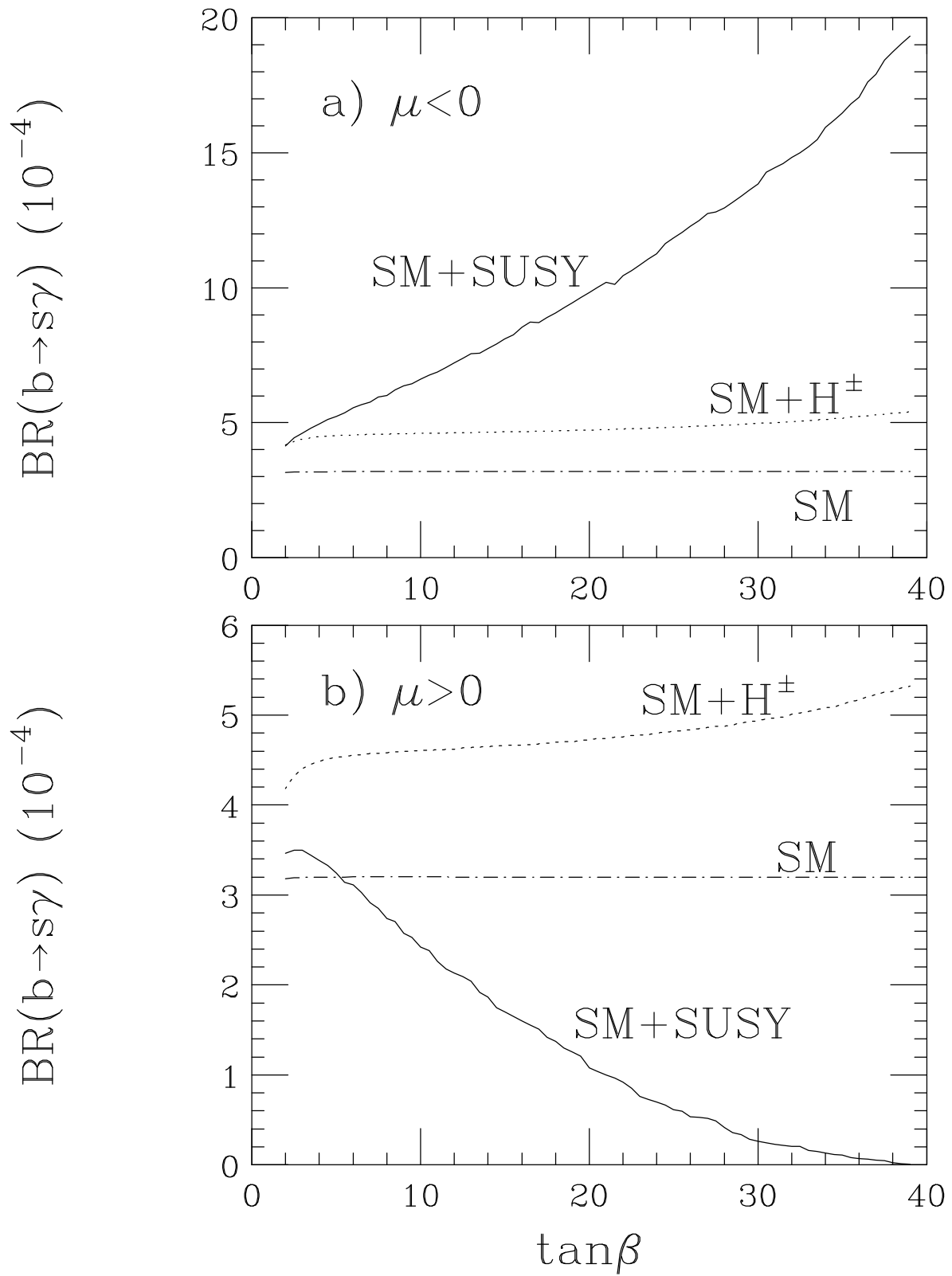


Fig. 2

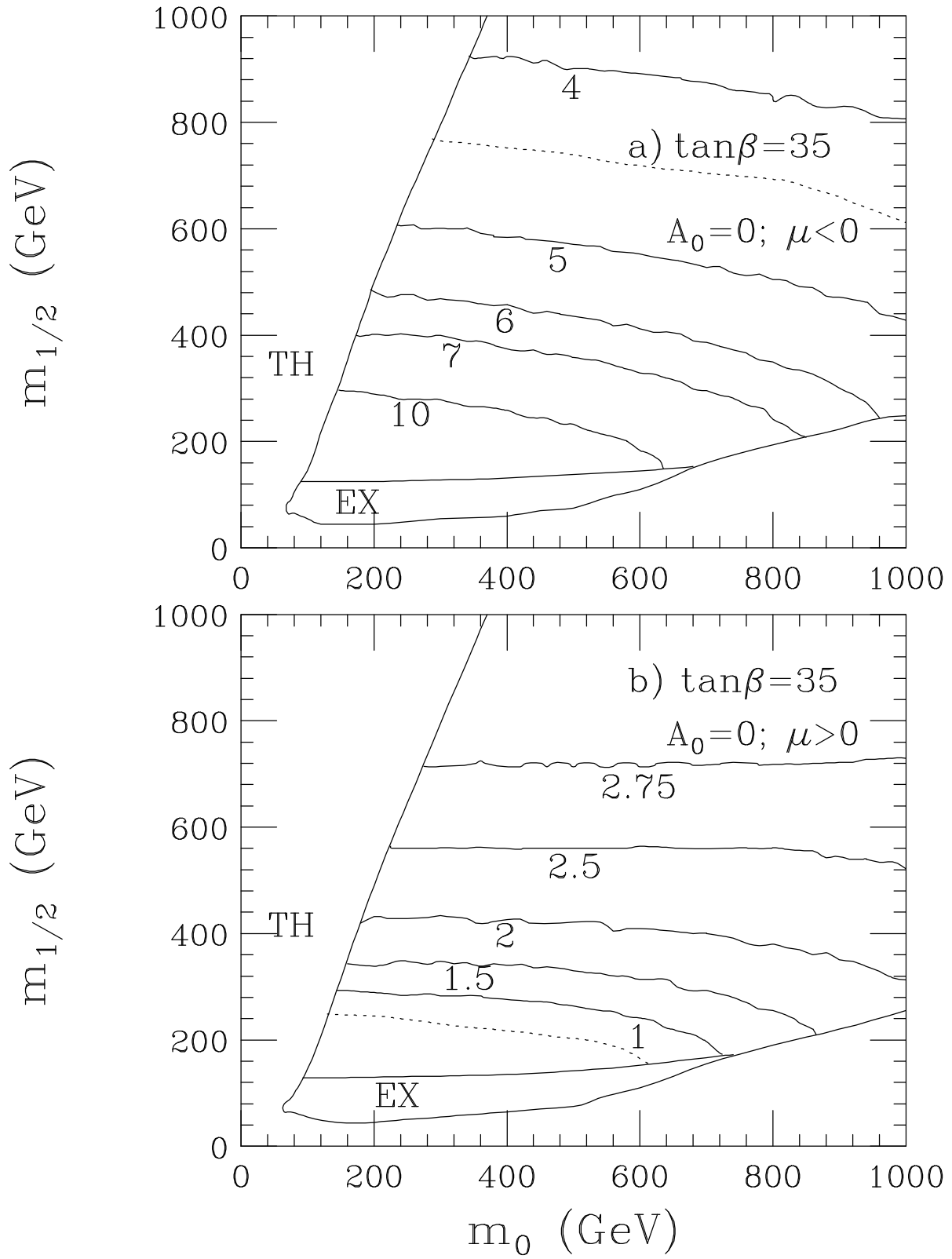


Fig. 3

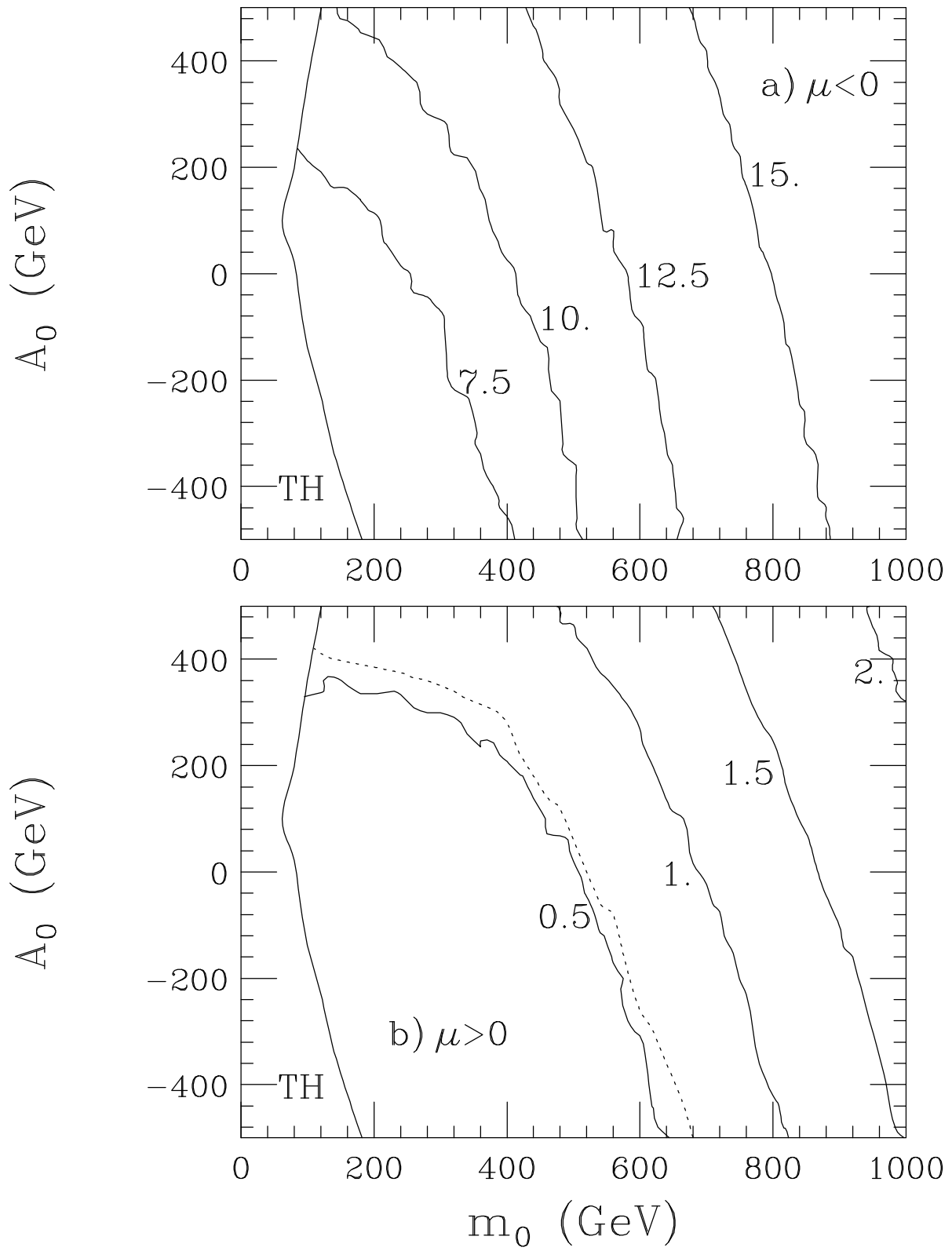


Fig. 4

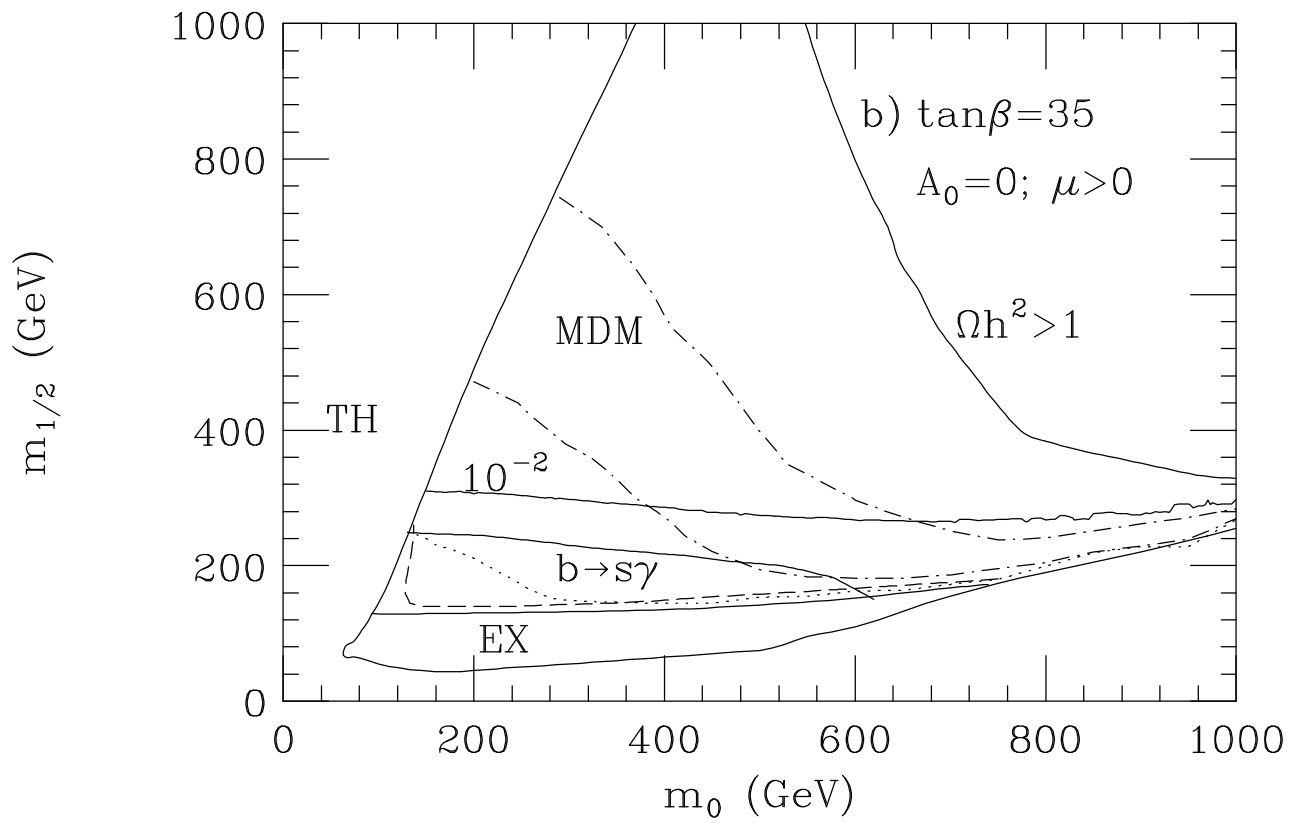
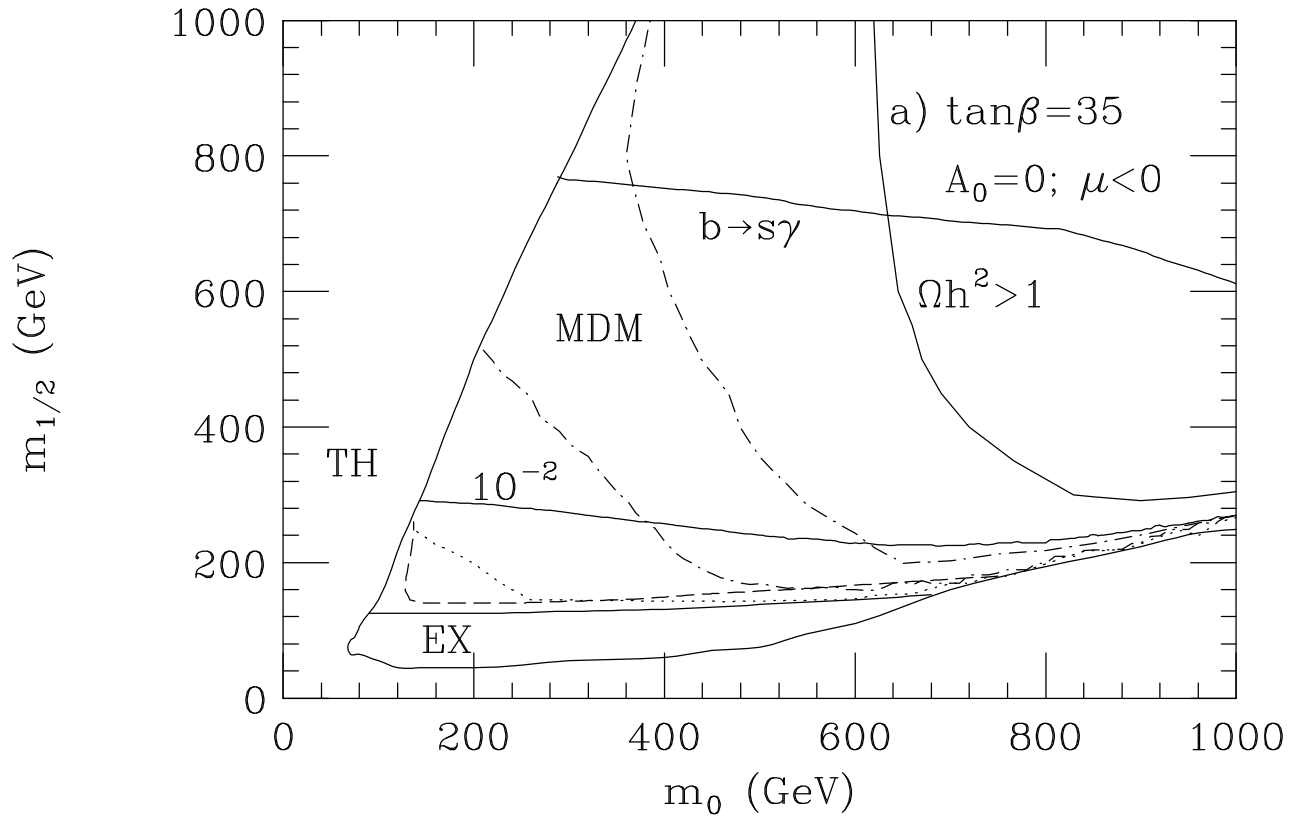


Fig. 5

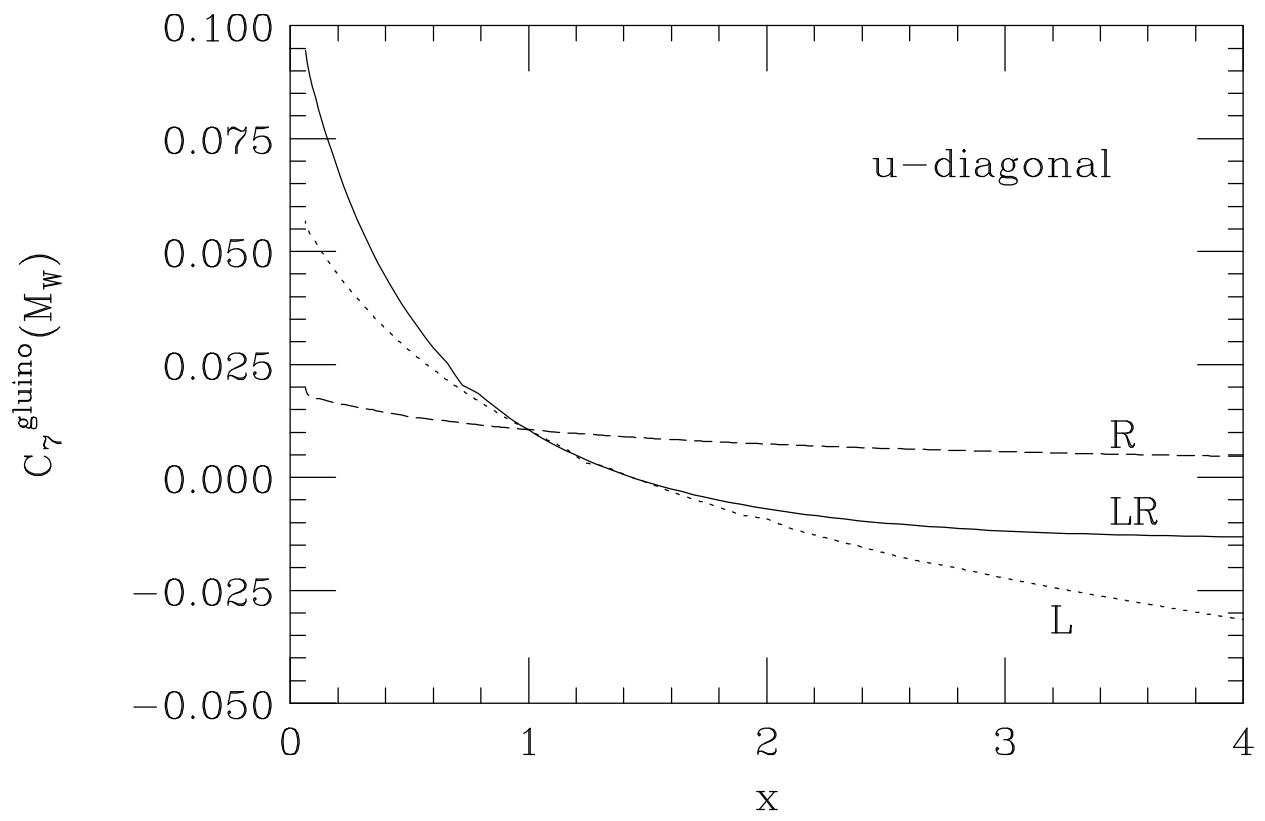
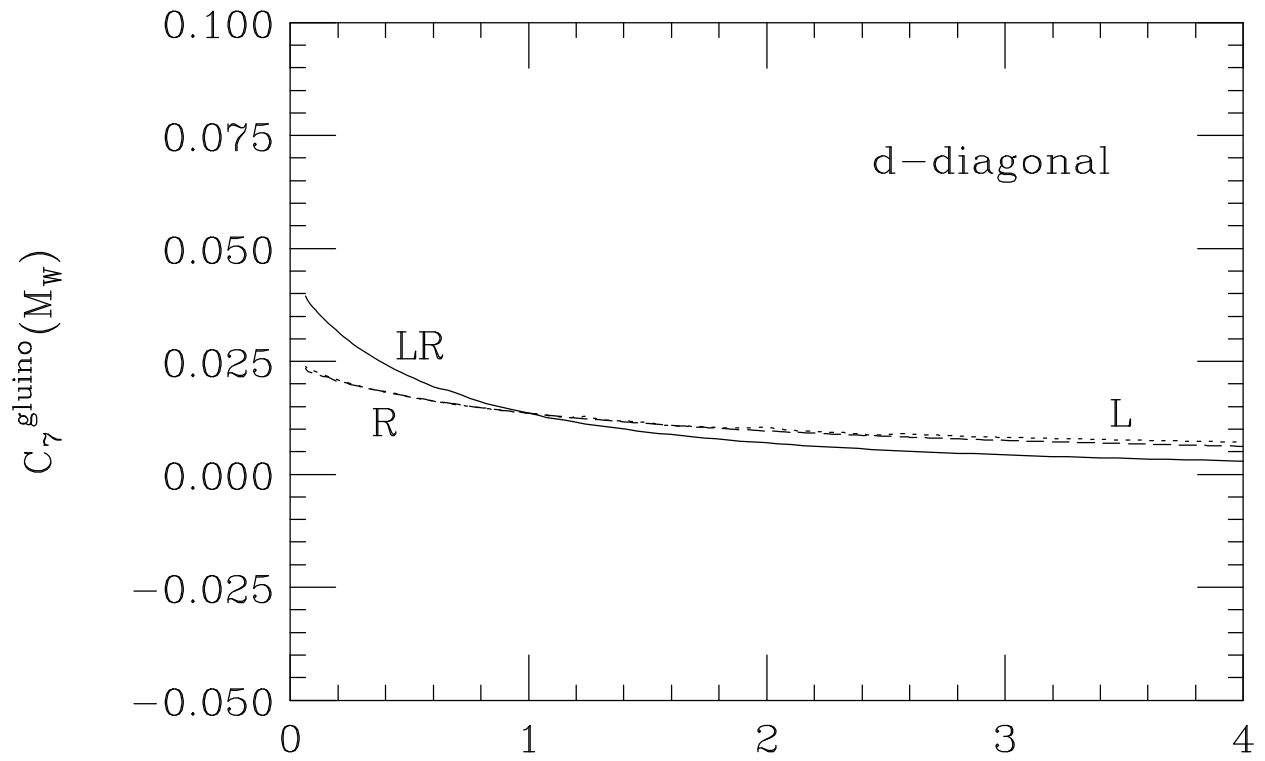


Fig. 6